

Strong Coupling Approach to the Supersymmetric Kondo Model.

P. Coleman ¹ , C. Pépin ² and A. M. Tsvelik ²

¹ *Materials Theory Group, Department of Physics and Astronomy, Rutgers University, 136*

Frelinghausen Road, Piscataway, NJ 08854, USA

² *Department of Physics, Oxford University, 1 Keble Road, Oxford OX1 3NP, UK*

Abstract

We carry out the strong coupling expansion for the $SU(N)$ Kondo model where the impurity spin is represented by a L-shaped Young tableau. Using second order perturbation theory around the strong coupling fixed point it is shown that when the antisymmetric component of the Young-tableau contains more than $N/2$ entries, the strong-coupling fixed point becomes unstable to a two-stage Kondo effect. By comparing the strong coupling results obtained here with the result using a supersymmetric large N expansion, we are also able to confirm the validity of the the supersymmetric formalism for mixed symmetry Kondo models.

78.20.Ls, 47.25.Gz, 76.50+b, 72.15.Gd

Typeset using REVTeX

In this paper we present a strong-coupling treatment of a single-impurity Kondo model where the spin is a higher representation of the group $SU(N)$. We consider spin representations that can be tuned continuously from being antisymmetric to being fully symmetric. This work is motivated in part by a desire to understand how the presence of strong Hund's interactions between electrons modify the spin quenching process. These issues become particularly important in heavy electron systems, where the localized electrons can be subject to Hund's interactions which far exceed their kinetic energy.^{1,2}

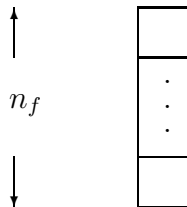
The basic model of interest is the single-site Kondo model, described by the Hamiltonian

$$H = \sum \epsilon_k c_{k\sigma}^\dagger c_{k\sigma} + \frac{J}{N} c_\alpha^\dagger(0) \mathbf{\Gamma}_{\alpha\beta} c_\beta(0) \cdot \mathbf{S}. \quad (1)$$

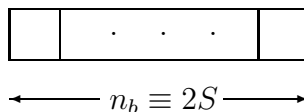
Here, the spin sums run over $N > 1$ possible values, $c_\alpha^\dagger(0) = \frac{1}{\sqrt{n_s}} \sum_k c_{k\alpha}^\dagger$ creates an electron at the origin, n_s is the number of sites. The matrices $\mathbf{\Gamma} = (\Gamma^1, \Gamma^2 \dots)$ are the form a basis of $N^2 - 1$ traceless $SU(N)$ matrices, where $\text{Tr}[\Gamma^a \Gamma^b] = \delta^{ab}$ and $\mathbf{S} = (S^1, S^2 \dots)$ is a spin describing a particular representation of $SU(N)$. The above model was first derived by Coqblin and Schrieffer⁵, who showed that a rare earth ion containing a single, spin-orbit coupled f-electron corresponds to the above model, with $N = 2j + 1$, and the spin in the fundamental representation of $SU(N)$.

When we come to consider more complex local moment systems, we need to consider the atomic spins formed by combining more than one elementary spin. Previous treatments of this model have considered local moments described by symmetric or antisymmetric representations of $SU(N)$, denoted by the Young tableaux⁶

(a) Antisymmetric



(b) Symmetric



The first representation describes n_f elementary spins that have been combined into a purely antisymmetric spin wavefunction; the second describes $n_b \equiv 2S$ elementary spins that have been combined into a purely symmetric spin wavefunction. These two representations are of particular interest because the former can be described by a combination of n_f spin, or “Abrikosov” pseudo fermions, whereas the latter can be described by a combination of $n_b \equiv 2S$ “Schwinger bosons”, and is the natural generalization of spin-S to $SU(N)$. For a given number of spins, the antisymmetric and symmetric spin combinations represent two extremes where the “Casimir” \mathbf{S}^2 attains its extremal values. Loosely speaking, the antisymmetric and symmetric spin representations are the combination of spins with the smallest and largest total spin, respectively. The symmetric spin configuration can thus be thought of as a state where a large Hund’s coupling has maximized the total spin.

The “column -shaped” representations of the $SU(N)$ Kondo model have been considered by previous authors in various contexts. The $SU(N)$ Kondo model in its fundamental representation has been treated using both Bethe ansatz^{7,8} and later in the context of a path integral large N expansion⁹. Later work lead to the realization that higher antisymmetric “column” representations of the same model are required for a well-defined large N expansion^{10,11}. The introduction of conformal field theory¹² showed how this could be used to compute spin correlation functions in both the single and multi-channel models. More recently, row¹³ and then column¹⁴ representations of $SU(N)$ of the multi-channel Kondo model have also been considered using both large N and conformal field theory methods. In all of these cases, screening of the local moment involves a single Kondo energy scale, independently of whether the moment is screened, underscreened or overscreened.

In this paper, we are interested in a new class of “L-shaped” spin representations composed of spins which interpolate between row and column representations, as shown in Fig 1. below This family of representations enables us to examine the effect of progressively turning on the Hund’s interaction the effect of progressively increasing the strength of the Hund’s interaction between the constituent spins inside an atom. In are a real multi-electron local moment, such as a U^{3+} ion, containing three localized f – electrons, the Hund’s interaction

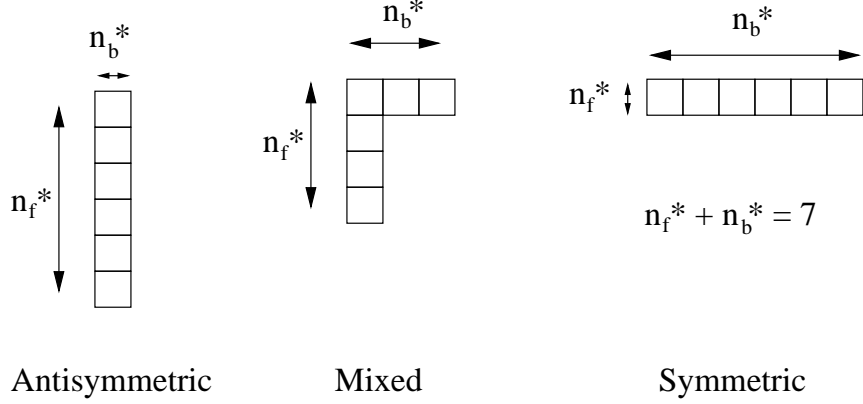


FIG. 1. A sequence of L-shaped Young tableaux which interpolate between antisymmetric and symmetric representation. Each tableau has six boxes, corresponding to six elementary spins.

also imposes the crystalline symmetry, leading to a model with a far lower symmetry. Our toy representation enables us to separate the leading order effect of the Hund’s interaction from the additional complications of lowering the symmetry.

In a previous paper³, we showed that the above mixed symmetry representations of $SU(N)$ spins can be described using a “super-symmetric spin” representation. In particular, if b_α^\dagger and f_α^\dagger ($\alpha = (1, N)$) are bose and Fermi creation operators, respectively, then a mixed symmetry representation of is obtained by writing the spin \mathbf{S} as a sum of a bosonic and a fermionic spin

$$\mathbf{S} = b_\alpha^\dagger \mathbf{\Gamma}_{\alpha\beta} b_\beta + f_\alpha^\dagger \mathbf{\Gamma}_{\alpha\beta} f_\beta \quad (2)$$

where $\mathbf{\Gamma} \equiv (\Gamma^1, \dots, \Gamma^M)$ represents the $M = (N^2 - 1)/2$ independent $SU(N)$ generators. In this way, the spin representation combines aspects of the bosonic “Schwinger boson” representation of spins and the fermionic “Abrikosov pseudo-fermion” representation of spins. This spin operator commutes with the the operators

$$\theta^\dagger = \sum_{\beta=1,N} f_\beta^\dagger b_\beta, \quad \theta = \sum_{\beta=1,N} b_\beta^\dagger f_\beta. \quad (3)$$

These operators interconvert the bose and fermion fields and form the generators of the supergroup $SU(1|1)$. An irreducible L-shaped representation of $SU(N)$ is obtained by imposing two constraints

$$\begin{aligned}\hat{n}_f + \hat{n}_b &= Q, \\ \hat{n}_f - \hat{n}_b + \frac{1}{Q}[\theta^\dagger, \theta] &= Y,\end{aligned}\tag{4}$$

where Q and Y are determined from the Young tableau via the relations $Q = n_f^* + n_b^*$ and $Y = n_f^* - n_b^*$. These constraints also commute with the generators θ and θ^\dagger , so the entire spin representation is supersymmetric.

This mixed representation of the spin-operators allows a consideration of the properties of Kondo models with L-shaped Young-tableaux by developing a supersymmetric field theory and then carrying out a large- N expansion. In the conventional one-channel Kondo model, the spin is screened from S to $S - \frac{1}{2}$ by a process that is characterized by a single temperature scale, the Kondo temperature. In the classic picture, this leads to a screening cloud of dimension $l = v_F/T_K$, where v_F is the Fermi velocity of electrons in the conduction sea and T_K is the single Kondo temperature. One of the unexpected results of the new analysis, was that under some circumstances a local moment under the influence of a Hund's interaction can undergo a two-stage Kondo effect associated with two separate Kondo temperatures T_{K1} and T_{K2} , leading to a screening cloud with ‘‘internal structure’’, characterized by two screening length scales

$$l_1 = \frac{v_F}{T_{K1}}, \quad l_2 = \frac{v_F}{T_{K2}}\tag{5}$$

where v_F is the Fermi velocity of the electrons, as illustrated in Fig. 2. In the language of the renormalization group, a new fixed point occurs where the impurity is screened in two stages reducing the effective spin from S to $S^* = S - 1$, where $2S = n_b^*$ and $2S^*$ are the width of the Young Tableau for the bare and the partially screened local moment, respectively. In this paper we provide a complimentary ‘‘strong-coupling’’ treatment of the same model. Our results confirm the key results obtained in the large N expansion, providing an important check on the validity of the supersymmetric field theory.

It is well known that under the renormalization group, the antiferromagnetic Kondo model renormalizes towards strong coupling^{15,16}. The weak-coupling beta function for the

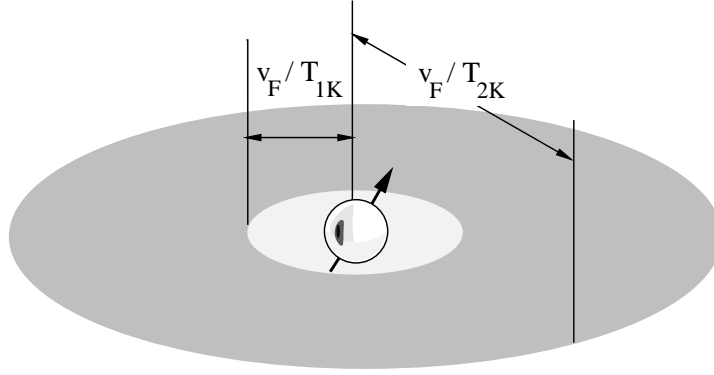


FIG. 2. Illustrating a local moment that is screened by a two-stage screening process in a single scattering channel. The screening cloud contains a “shell structure”, with an inner and outer conduction electron cloud which reduce the total moment from S to $S^* = S - 1$.

Kondo model is independent of representation, and for a single channel model, takes the form

$$\beta(g) = \frac{dg(\Lambda)}{d\Lambda} = -g^2 + \frac{g^3}{N} + O(g^4) \quad (6)$$

where $g = J\rho$ and ρ is the conduction electron density of states. For the simplest one-channel Kondo models, the coupling constant g flows smoothly from the unstable weak-coupling fixed point, to a stable strong coupling fixed point. However, in certain cases the strong coupling fixed point is itself unstable. The most famous example of such behaviour is the two-channel Kondo model, where the flow to strong coupling is intercepted by an intermediate coupling fixed point that is characterized by a non fermi liquid properties^{4,17,18}. The two stage Kondo effect discussed here is another example of an instability at strong coupling. As we shall see, the strong coupling fixed point becomes unstable to a second Kondo effect at an exponentially smaller temperature.

The classic analysis⁴ of the stability of the strong coupling fixed point of a Kondo model follows Wilson’s method¹⁹ of formulating the Kondo model on a lattice:

$$H = -t \sum_{n \geq 1, \alpha} [c_{\alpha}^{\dagger}(n+1)c_{\alpha}(n) + \text{H.c}] + \frac{J}{N} c_{\alpha}^{\dagger}(0) \mathbf{\Gamma}_{\alpha\beta} c_{\beta}(0) \cdot \mathbf{S} \quad (7)$$

The strong-coupling fixed point is obtained by first setting $t = 0$, and solving for the ground-state of the one-site problem

$$H_K = \frac{J}{N} c_\alpha^\dagger(0) \mathbf{\Gamma}_{\alpha\beta} c_\beta(0) \cdot \mathbf{S} \quad (8)$$

which leads to a partially screened local moment with spin S^* . When a finite t/J is restored, virtual charge fluctuations of electrons onto, and off site 0 induce an effective interaction between the spin density at site 1 and the residual moment, given by

$$H^{(1)} = J^* \mathbf{S}^* \cdot c_\alpha^\dagger(1) \mathbf{\Gamma}_{\alpha\beta} c_\beta(1) \quad (9)$$

where $J^* = O(t^2/J)$ determines the strength of the coupling between the residual local moment and the conduction electron at site 1. The stability of the strong coupling fixed point is determined by the sign of J^* . If this coupling is ferromagnetic ($J^* < 0$), then a residual ferromagnetic Kondo effect with the low energy electrons causes J^* to scale logarithmically to zero, decoupling the residual spin from the conduction sea and stabilizing the strong-coupling fixed point. Conversely if the effective coupling is antiferromagnetic ($J^* > 0$), then the effective model flows to strong coupling and the strong coupling fixed point of the initial Kondo model becomes unstable.

To get a better idea of how antiferromagnetic coupling can arise in our *single-channel* model, consider a local moment, described by an L-shaped representation of $SU(N)$, denoted by the Young Tableau

$$\mathbf{S} = \begin{array}{c} \leftarrow 2S \rightarrow \\ \uparrow \\ \begin{array}{|c|c|c|c|c|} \hline \square & \square & \square & \square & \square \\ \hline \square & & & & \\ \hline \square & & & & \\ \hline \square & & & & \\ \hline \end{array} \\ \downarrow \\ n_f^* \end{array} \quad (10)$$

where we have replaced $n_b^* = 2S$. In the ground-state of the strong-coupling Hamiltonian H_K , electrons form a singlet with the fermionic part of the spin creating a partially screened moment, denoted by a Young-tableau with a completely filled first row.

$$\mathbf{S}^* = (\mathbf{\Gamma}_e(0) + \mathbf{S}) = \begin{array}{c} \begin{array}{c} \leftarrow 2S \rightarrow \\ \boxed{} \boxed{} \boxed{} \boxed{} \boxed{} \\ \uparrow \\ \boxed{} \\ \boxed{} \\ \boxed{} \\ \boxed{} \\ \boxed{} \\ \boxed{c_0} \\ \boxed{c_0} \\ \boxed{c_0} \\ \downarrow \\ N \end{array} \\ \equiv \\ \begin{array}{c} \leftarrow 2S - 1 \rightarrow \\ \boxed{} \boxed{} \boxed{} \boxed{} \end{array} \end{array} \quad (11)$$

where in this example we have taken $N = 8$. Since the first column of the tableau is a singlet (with N boxes), it can be removed from the tableau, leaving behind a partially screened spin $S - 1/2$, described by a row with $2S - 1$ boxes. If we now couple the electron at the origin with electrons at site '1' via a small hopping matrix element $t \ll J$, then the virtual charge fluctuations of electrons in and out of the singlet at the origin will lead to a residual coupling between the partially screened moment and the electrons at the neighboring site '1'

$$H^{(1)} = J^* \mathbf{S}^* \cdot c_\alpha^\dagger(1) \mathbf{\Gamma}_{\alpha\beta} c_\beta(1) \quad (12)$$

where $J^* \sim t^2/J$. In the SU(2) Kondo model, only electrons parallel to the residual moment \mathbf{S}^* can hop onto the origin, which gives rise to a ferromagnetic coupling $J^* < 0$. In the SU(N) case, electrons can hop provided they are not in the same spin state as electrons at the origin. The sign of the coupling J^* depends on the number of conduction electrons $n_c = N - n_f^*$, bound at the origin. For example, if $n_f^* = 1$, so that $n_c = N - 1$ in the ground state, electrons hopping onto the origin will have to be parallel to the residual spin, so in this case the coupling is ferromagnetic, $J^* < 0$. By contrast, if $n_c \ll N$, there are many ways for the electron to hop onto the origin with a spin component that is different to the residual moment, so the residual interaction will be antiferromagnetic, $J^* > 0$. In this case, the the strong-coupling fixed point becomes unstable, and a second-stage Kondo effect occurs, binding a further $N - 1$ electrons at site "1" to form a state represented by the tableau

$$\mathbf{S}^{**} = (\mathbf{\Gamma}_{e_0} + \mathbf{\Gamma}_{e_1} + \mathbf{S}) = \begin{array}{c} \begin{array}{c} \leftarrow 2S \rightarrow \\ \begin{array}{|c|c|c|c|} \hline & & & \\ \hline & c_1 & & \\ \hline & c_1 & & \\ \hline & c_1 & & \\ \hline & c_1 & & \\ \hline c_0 & c_1 & & \\ \hline c_0 & c_1 & & \\ \hline c_0 & c_1 & & \\ \hline \end{array} \\ \begin{array}{c} \uparrow \\ N \\ \downarrow \end{array} \end{array} \equiv \begin{array}{c} \begin{array}{|c|c|c|} \hline & & \\ \hline & & \\ \hline & & \\ \hline \end{array} \\ \begin{array}{c} \leftarrow 2S - 2 \rightarrow \\ \begin{array}{|c|c|c|} \hline & & \\ \hline & & \\ \hline & & \\ \hline \end{array} \end{array} \end{array} \quad (13)$$

which corresponds to a residual spin $S^{**} = S - 1$. This final configuration is stable, because an electron at site "2" can only hop onto site "1" if it is parallel to the unquenched moment, so the residual interaction between site "2" and site "1" will be ferromagnetic.

To examine the stability of the strong coupling fixed point in detail, this paper follows the method of Nozières and Blandin⁴, using second order perturbation theory about the strong-coupling fixed point to determine the sign of the residual interaction between the unscreened spin and the bulk of conduction electrons. If $J^* < 0$ the residual coupling is ferromagnetic and the strong coupling fixed point is stable: the impurity residual spin is $S^* = S - 1/2$ after screening. If $J^* > 0$ the residual interaction is antiferromagnetic and the strong coupling fixed point becomes unstable, leading to the two-stage Kondo effect $S^* = S - 1$. In parallel with this approach, we carry out a large N treatment of the strong-coupling limit, using the technique developed in our previous paper. By comparing the two techniques we are able to confirm the validity of the field theoretic approach developed in our earlier work. Both methods are able to confirm that for $N > 2$, J^* changes sign when the number of bound-conduction electrons is less than $N/2$, and in the large N limit is given by

$$J^* = -\frac{t^2}{J(1 - \tilde{n}_f)\tilde{n}_f} \left[\frac{\frac{1}{2} - \tilde{n}_f}{(1 - \tilde{n}_f + \tilde{n}_b)} \right] \quad (14)$$

where $\tilde{n}_f = n_f/N$ and $\tilde{n}_b = 2S/N$.

The table below gives a shows the main results, comparing the strong coupling and large N expressions for the ground-state energy E_g , the excitation energie $\Delta E^{\uparrow\uparrow}$ and $\Delta E^{\uparrow\downarrow}$ to add an electron to the ground state in a spin configuration that is "parallel" or "anti-parallel"

to the residual spin. The last row compares the effective coupling constant J^* calculated by both methods. In these expressions, we denote $\tilde{n}_f = n_f^*/N$, $\tilde{n}_b = n_b^*/N$, $q = Q/N$.

	Strong Coupling	Large N
Ground State Energy E_g	$-NJ[(1 - \tilde{n}_f)(\tilde{n}_f + q/N)]$	$-NJ(1 - \tilde{n}_f)\tilde{n}_f$
$\Delta E^{\uparrow\downarrow} = E^{\uparrow\downarrow}(n_e + 1) - E_g$	$J(1 - \tilde{n}_f - q/N)$	$J(1 - \tilde{n}_f)$
$\Delta E^{\uparrow\uparrow} = E^{\uparrow\uparrow}(n_e + 1) - E_g$	$J(1 - \tilde{n}_f + \tilde{n}_b - q/N)$	$J(1 - \tilde{n}_f + \tilde{n}_b)$
Effective coupling constant	$\frac{t^2}{(2S)J} \left[\frac{n_f N}{(N-1)(N-n_f^*-Q/N)} - \frac{QN}{(Q+Nn_f^*)(1+N+Q-2n_f^*-Q/N)} - \frac{(N-n_f^*)(Q-n_f^*)N}{(N-1)(Q+N-n_f^*)(n_f^*+Q/N)} \right]$	$\frac{t^2(1/2 - \tilde{n}_f)}{J(1 - \tilde{n}_f)\tilde{n}_f(1 - \tilde{n}_f + \tilde{n}_b)}$

I. THE ONE SITE IMPURITY PROBLEM

To begin, we start with the one-dimensional rendition of the SU(N) Kondo model,

$$H = -t \sum_{n \geq 0, \alpha} \left[c_\alpha^\dagger(n+1)c_\alpha(n) + \text{H.c.} \right] + \frac{J}{N} c_\alpha^\dagger(0) \mathbf{\Gamma}_{\alpha\beta} c_\beta(0) \cdot \mathbf{S} \quad (15)$$

where $c_\alpha^\dagger(j)$ creates an electron at the site of the local moment, \mathbf{S} is the spin of the local moment and $\mathbf{\Gamma}_{\alpha\beta}$ is a generator of the SU(N) group. For simplicity we have put the impurity at the beginning of the chain. The spin of the impurity is represented by an L-shaped Young tableau while the conduction electron is represented with a single box.

In the strong coupling limit, only the local part of the hamiltonian is relevant and the problem becomes single sited. In order to determine what is the ground state of the single site problem, we consider the impurity described by a Young Tableau with Q boxes. In order to simplify further calculations, we denote by n_b the number of boxes in the row and by n_f the number of boxes in the column minus one. (This will correspond in the next section to put some bosons in the row as well as in the corner and to fill the remaining of

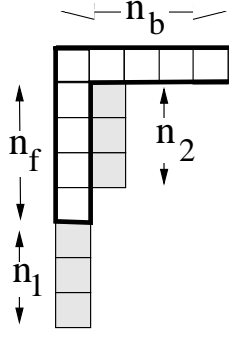


FIG. 3. Screening of the impurity. n_1 and n_2 denote the number of conduction electrons screening the impurity in the first and second column of the Young tableau.

the column with fermions.) In the strong coupling limit, the conduction electrons will be trapped at the impurity site, screening the impurity. We note n_1 and n_2 the number of conduction electrons screening the impurity respectively in the first and second column of the Young Tableau (see Fig. 3).

The energy of the ground state can be expressed in terms of second order Casimirs

$$\begin{aligned}
 E &= \frac{J}{N} \mathbf{S}_c \cdot \mathbf{S}_i \\
 &= \frac{J}{2N} [\mathbf{S}_{tot}^2 - \mathbf{S}_i^2 - \mathbf{S}_c^2] ,
 \end{aligned} \tag{16}$$

where \mathbf{S}_{tot}^2 is the second order Casimir of the impurity screened by the $n_1 + n_2$ conduction electrons; \mathbf{S}_i^2 is the Casimir of the free impurity and \mathbf{S}_c^2 is the Casimir of the conduction electrons which screen the impurity.

If we normalize the generators of the fundamental representation of $SU(N)$ according to $Tr[\Gamma^\alpha \Gamma^\beta] = \delta^{\alpha\beta}$, then the expression for the Casimir of an arbitrary irreducible representation is²⁰

$$\mathbf{S}^2 = \frac{Q(N^2 - Q)}{N} + \sum_{j=1, N} m_j (m_j + 1 - 2j) , \tag{17}$$

where $m - j$ is the number of boxes in the j -th row from the top. The energy of the ground state is then given by

$$E = \frac{J}{2N} [2n_2 (N - n_2) + (n_f + n_1 - n_2) (N - n_f - n_1 - n_2 - 1)]$$

$$\begin{aligned}
& - \frac{1}{N} (Q + n_1 + n_2)^2 - n_f (N - n_f - 1) + \frac{1}{N} Q^2 \\
& - (n_1 + n_2) (N + 1 - n_1 - n_2) + \frac{1}{N} (n_1 + n_2)^2 \Big]. \quad (18)
\end{aligned}$$

The energy in the $[n_1, n_2]$ plane has the form represented in figure 4. In the range of

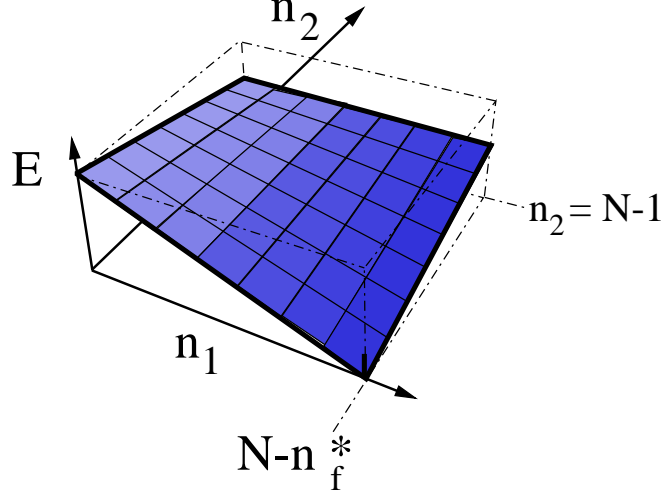


FIG. 4. Single impurity energy as a function of the parameters n_1 and n_2 . We see that the minimum is given when n_1 is maximum ($n_1 = N - n_f - 1$) and n_2 is minimum ($n_2 = 0$).

parameters we are interested in ($n_1 \in [0, N - n_f - 1]$, $n_2 \in [0, N - 1]$), only one minimum remains and the ground state of the problem is found to be

$$n_1 = N - n_f - 1 \quad ; \quad n_2 = 0 \quad (19)$$

which corresponds to the usual one-stage Kondo model where the impurity spin is screened by $1/2$.

A special exception to this case occurs when $Q/N = k$ is an integer, when, if $n_1 = Q/N = k$, $\frac{\partial E}{\partial n_2} = 0$ for all n_2 . The point $n_1 = Q/N = k$, $n_2 \in [1, N - 1]$ corresponds to a line of degenerate ground states. An example is illustrated on figure 5. In this case, the strong coupling fixed point is also unstable, but the fixed point physics will be governed by valence fluctuations between the degenerate states of different n_2 . We shall exclude this special case from the discussion here, leaving it for future work.

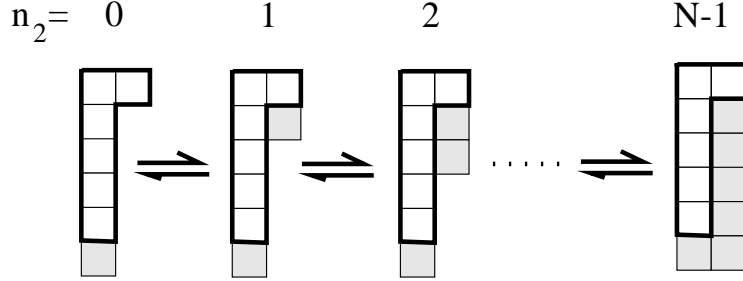


FIG. 5. In the special case where $Q/N = k$ is an integer and $n_1 = k$, it costs no energy to add additional electrons to the ground-state and the fixed point behavior of this particular Kondo model will then involve valence fluctuations between the different degenerate configurations. The figure illustrates the situation where $Q = N = 6$ and $n_1 = 1$.

II. SECOND ORDER PERTURBATION THEORY AROUND THE STRONG COUPLING FIXED POINT

In the leading order in $\frac{1}{J}$ two processes of excitation appear. Suppose the screened impurity is at site “zero”. Then one electron from site “one” can hop briefly to site zero, then return (process 1). Alternatively one electron from site “zero” can make a virtual hop

Process I.

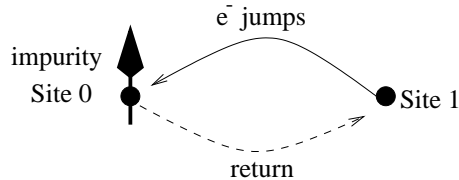


FIG. 6. Process I: an electron makes a virtual incursion from site 1 onto site 0.

to site one and return (process 2). In the first process the intermediate state has one more electron at site one ($n_c + 1$), where n_c is the number of conduction electrons which screen the impurity in the ground state). We note this state $|GS + 1, 0\rangle$. In the second process of excitations the intermediate state has $n_c - 1$ electron at site zero and two electrons at site one. We note it $|GS - 1, 2\rangle$. If we call $|GS, 1\rangle$ the initial state (the site 0 has the impurity in the ground state and the site 1 has one electron), then using second order perturbation

Process II.

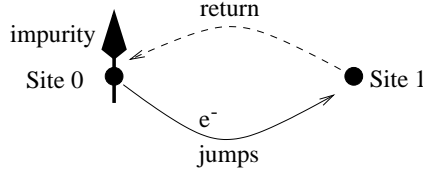


FIG. 7. Process II : an electron at site zero makes a virtual incursion to to site 1.

theory, the energy shift due to the perturbation is given by

$$\begin{aligned} \Delta E = t^2 & \frac{|\langle GS + 1, 0 | c_1^\dagger c_2 | GS, 1 \rangle|^2}{E(n_e) - E(n_e + 1)} \\ & + t^2 \frac{|\langle GS - 1, 2 | c_2^\dagger c_1 | GS, 1 \rangle|^2}{E(n_e) - E(n_e - 1)}, \end{aligned} \quad (20)$$

where $E(n_e)$ is the energy of the initial state; $E(n_e + 1)$ is the energy of the intermediate state in process 1 and $E(n_e - 1)$ is the energy of the intermediate state in process 2.

Now for each process of excitation the spin of the electron at site 1 can is either symmetrically (Fig. 8 (a)), or antisymmetrically (Fig. 8 (b)) correlated with the spin at the impurity. For SU(2) spins, this corresponds to a spin that is either “parallel” or “anti-parallel” to the impurity spin, and we shall adopt the same convention for the SU(N) case. There are two corresponding possibilities for the energy shifts

$$\begin{cases} \Delta E^{\uparrow\uparrow} = \frac{M_{(1)}^{\uparrow\uparrow}}{E(n_e) - E^{\uparrow\uparrow}(n_e + 1)} + \frac{M_{(2)}^{\uparrow\uparrow}}{E(n_e) - E(n_e - 1)}, \\ \Delta E^{\uparrow\downarrow} = \frac{M_{(1)}^{\uparrow\downarrow}}{E(n_e) - E^{\uparrow\downarrow}(n_e + 1)} + \frac{M_{(2)}^{\uparrow\downarrow}}{E(n_e) - E(n_e - 1)} \end{cases}, \quad (21)$$

where for example $M_{(1)}^{\uparrow\uparrow}$ and $M_{(1)}^{\uparrow\downarrow}$ are the matrix elements for process one in the parallel and antiparallel configurations, respectively.

Supposing now that the effective Hamiltonian around the strong coupling fixed point takes the form

$$H^{(1)} = J^* \mathbf{S}^* \cdot c_\alpha^\dagger(1) \mathbf{\Gamma}_{\alpha\beta} c_\beta(1) \quad (22)$$

by computing the energy difference between the parallel and anti-parallel configurations, the effective Kondo coupling constant is then

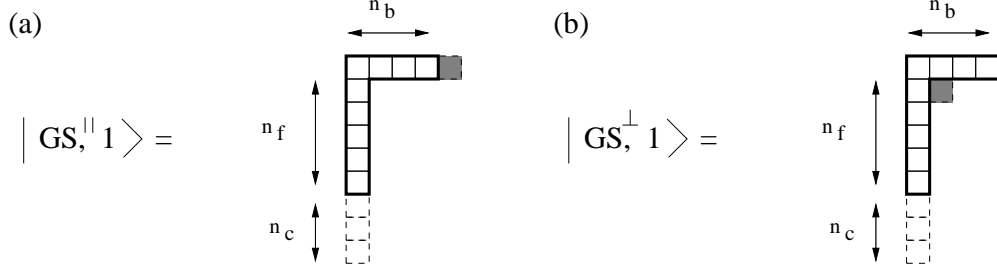


FIG. 8. (a) “Parallel” configuration: the spin of the electron at site 1 is symmetrized with the impurity spin. (b) “Anti-Parallel” configuration: the spin of the electron at site 1 is anti-symmetrized with the impurity spin.

$$\Delta E^{\uparrow\uparrow} - \Delta E^{\uparrow\downarrow} = J_{eff}(2S). \quad (23)$$

Thus by evaluating the energy shifts in the second order perturbation theory we are able to determine the sign and hence the stability of the fixed point.

A. Evaluation of the energies

First, consider the energy of the ground state at site one. It is given by

$$E(n_e) = -\frac{J}{N} [(N-1-n_f)(n_f + (N+Q)/N)]. \quad (24)$$

Suppose now one electron jumps from site 1 to site 0 in the “parallel” state, as in figure 8 (a), the the energy of the intermediate state is

$$E^{\uparrow\uparrow}(n_e) = \frac{J}{2N} [\mathbf{S}_{N+1}^2 - \mathbf{S}_{imp}^2 - \mathbf{S}_{el}^2]$$

where \mathbf{S}_{N+1}^2 is the Casimir of the intermediate state; \mathbf{S}_{imp}^2 is the Casimir of the impurity before screening and \mathbf{S}^2 is the Casimir of all $(n_c + 1)$ conduction electrons involved into the intermediate state. The resulting energy is given by

$$E^{\uparrow\uparrow}(n_e + 1) = -\frac{J}{N^2} [n_f (N^2 - n_b - n_f - Nn_f)].$$

Similarly if the starting spin configuration is the “anti-parallel” one, as in 8 (b), the energy of the intermediate state is

$$E^{\uparrow\downarrow}(n_e + 1) = -\frac{J}{N} [n_b (1 - n_f/N) + n_f (N - n_f - n_f/N)] .$$

For process 2, the energy of the intermediate state does not depend on whether the spin configuration is parallel or anti-parallel, and is given by

$$E(n_e - 1) - E(n_e) = \frac{J}{N} (n_f + 1 + Q/N) .$$

In conclusion the two energy differences associated with process 1 are given by

$$\begin{cases} E^{\uparrow\downarrow}(n_e + 1) - E(n_e) = \frac{J}{N} (N - n_f^* - Q/N) \\ E^{\uparrow\uparrow}(n_e + 1) - E(n_e) = \frac{J}{N} (N - n_f^* + n_b^* - Q/N) \end{cases} \quad (25)$$

where we have replaced $n_f + 1 \rightarrow n_f^*$ and $n_b \rightarrow n_b^*$. The excitation energy associated with process 2 is

$$E(n_e - 1) - E(n_e) = \frac{J}{N} (n_f^* + Q/N) \quad (26)$$

for both spin configurations.

B. Matrix elements

The calculation of the matrix elements is much more complex and requires a detailed expression for each state involved in terms of operators. We will begin by introducing the notation, using the ground state as an example. Then we will review the matrix elements for each process of excitation.

1. Notation

The screened impurity in its ground state is given by the following Young Tableau represented in figure 9: Each box is filled with a field to which an index is attached. In order to describe the state we have to first symmetrize the indices of the fields in the row and then antisymmetrize the indices in the column. We choose to fill the row with $n_b = 2S$ bosons in a given spin state (say, all the bosons have index A), and the rest of the column will be

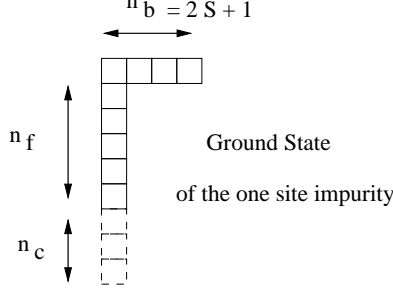


FIG. 9. Ground state after the screening of the impurity spin by conduction electrons. Note that we have changed our notations here and have given a spin $S + 1/2$ to the initial impurity spin. filled with $n_f = n_f^* - 1$ f-fermions and n_c conduction electrons so that $n_f^* + n_c = N$. With these conventions the ground state can be expressed as

$$\begin{aligned}
|GS\rangle = \frac{1}{N_{GS}} & \left[(b_A^\dagger)^{2S} \sum_{\mathcal{P}\{\sigma\} \in \{1\dots N\} - \{A\}} \varepsilon(\mathcal{P}) f_{\sigma_1}^\dagger \cdots f_{\sigma_{n_f}}^\dagger c_{\sigma_{n_f+1}}^\dagger \cdots c_{\sigma_{N-1}}^\dagger |0\rangle \right. \\
& \left. + \sum_{\sigma_i \neq A} (b_A^\dagger)^{2S-1} b_{\sigma_i}^\dagger \sum_{\mathcal{P}(\{\sigma\}) \in (\{1\dots N\} - \{\sigma_i\})} \varepsilon(\mathcal{P}) f_{\sigma_1}^\dagger \cdots f_{\sigma_{n_f}}^\dagger c_{\sigma_{n_f+1}}^\dagger \cdots c_{\sigma_{N-1}}^\dagger |0\rangle \right] \quad (27)
\end{aligned}$$

where $(\sigma_1 \dots \sigma_n) = \mathcal{P}(\alpha_1 \dots \alpha_n)$ are permutations of the set of indices $\{\alpha_1 \dots \alpha_n\}$ strictly ordered. $\varepsilon(\mathcal{P})$ is the sign of the permutation. N_{GS} is the normalization factor

$$N_{GS} = \sqrt{2S + N - 1} \binom{N - 1}{n_f}^{1/2} (2S - 1)! n_f! n_c!$$

where $\binom{b}{a}$ is the number of ways of choosing a elements out of a group of b possible choices and $n_c = (N - 1 - n_f)$. In all that follows we will lighten the notation by keeping track of the degenerescences in any expression of states. For example the state $|GS\rangle$ can be written

$$\begin{aligned}
|GS\rangle = \frac{1}{N_{GS}} & n_f! n_c! \left[(b_A^\dagger)^{2S-1} \sum_{\tilde{\mathcal{S}}_{n_f} \in \{1\dots N\} - \{A\}} \varepsilon' f_{\sigma_1}^\dagger \cdots f_{\sigma_{n_f}}^\dagger c_{\sigma_{n_f+1}}^\dagger \cdots c_{\sigma_{N-1}}^\dagger |0\rangle \right. \\
& \left. + \sum_{\sigma_i \neq A} (b_A^\dagger)^{2S-1} b_{\sigma_i}^\dagger \sum_{\tilde{\mathcal{S}}_{n_f} \in (\{1\dots N\} - \{\sigma_i\})} \varepsilon' f_{\sigma_1}^\dagger \cdots f_{\sigma_{n_f}}^\dagger c_{\sigma_{n_f+1}}^\dagger \cdots c_{\sigma_{N-1}}^\dagger |0\rangle \right] \quad (28)
\end{aligned}$$

where we suppose that the two sets of indices $(\sigma_1 \dots \sigma_{n_f})$ and $(\sigma_{n_f+1} \dots \sigma_{N-1})$ are ordered in a strictly increasing order. ε' is the sign of the residual permutation of indices due to the fact that the two sets of indices are not ordered with respect to each other. $\tilde{\mathcal{S}}_{n_f} \in \{2 \dots N\}$

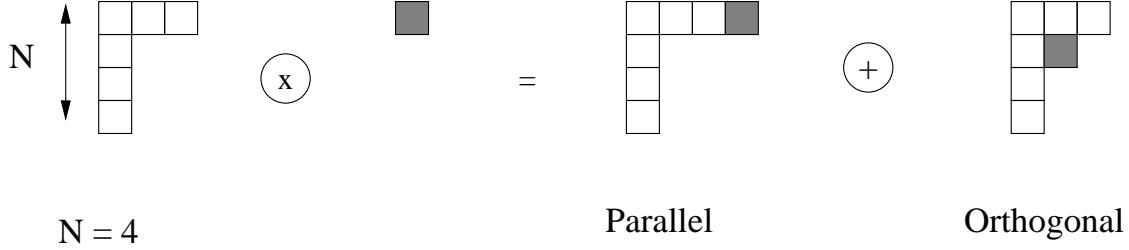


FIG. 10. Schematic tensor product between the screened impurity in the ground state and a conduction electron. Note that the number of boxes in the column of the screened impurity is N (the impurity is screened).

denotes the partition of the two sets of indices $(\sigma_1 \dots \sigma_{n_f})$ and $(\sigma_{n_f+1} \dots \sigma_{N-1})$ chosen among $\{2 \dots N\}$ and strictly ordered inside each set. The important point here is that the above sum runs over linearly independent states only. Thus when we have to evaluate the norm of a state, the prefactors in front of the sum have to be squared. We give in the Appendix the detailed evaluation of the norm of the ground state as an example.

2. Decomposition rule into parallel and anti-parallel states

When we add an additional electron to the ground-state, the state that forms is a linear combination of two states, one in which the spin is symmetrically correlated with the impurity, and another in which or antisymmetrically correlated with the partially screened impurity, as illustrated by the Young tableau 10). In the analogous $SU(2)$ problem, these two states would correspond to adding an electron into a state in which the spin that is either “parallel” or “anti-parallel” to the impurity spin. Written out in operator language, then if α is the spin index of the added electron,

$$\begin{aligned}
 c_\alpha^\dagger |GS\rangle &= \overbrace{\frac{1}{2S} (c_\alpha^\dagger |GS\rangle + (2S-1) c_A^\dagger |\varphi_{int}(\alpha)\rangle)}^{\text{parallel}} \\
 \oplus \overbrace{\frac{1}{2S} ((2S-1) c_\alpha^\dagger |GS\rangle - (2S-1) c_A^\dagger |\varphi_{int}(\alpha)\rangle)}^{\text{anti-parallel}} .
 \end{aligned} \tag{29}$$

$|\varphi_{int}(\alpha)\rangle$ is a state where the index α of the new box has been exchanged with the indices of the bosons in the ground state (here, remember, all the bosons have index A). In each case the spin index of the added electron is symmetrized, or anti-symmetrized with the the boson spin indices, leaving the indices of the first column untouched because this column is a filled singlet in the ground state. The state $|\varphi_{int}(\alpha)\rangle$ can be written

$$\begin{aligned}
|\varphi_{int}(\alpha)\rangle = & \frac{1}{N_{GS}} \left[\binom{N-1}{n_f} n_f! n_c! (b_A)^{2S-1} b_\alpha^\dagger \sum_{\tilde{S}_{n_f} \in \{1\dots N\} - \{A\}} \varepsilon' f_{\sigma_1}^\dagger \cdots f_{\sigma_{n_f}}^\dagger c_{\sigma_{n_f+1}}^\dagger \cdots c_{\sigma_{N-1}}^\dagger |0\rangle \right. \\
& + \sum_{\alpha_i \neq \{A, \alpha\}} \binom{N-1}{n_f} n_f! n_c! (b_A)^{2S-2} b_\alpha^\dagger b_{\alpha_i}^\dagger \sum_{\tilde{S}_{n_f} \in \{1\dots N\} - \{A\}} \varepsilon' f_{\sigma_1}^\dagger \cdots f_{\sigma_{n_f}}^\dagger c_{\sigma_{n_f+1}}^\dagger \cdots c_{\sigma_{N-1}}^\dagger |0\rangle \\
& \left. + \binom{N-1}{n_f} n_f! n_c! (b_A^\dagger)^{2S-2} (b_\alpha^\dagger)^2 \sum_{\tilde{S}_{n_f} \in \{1\dots N\} - \{A\}} \varepsilon' f_{\sigma_1}^\dagger \cdots f_{\sigma_{n_f}}^\dagger c_{\sigma_{n_f+1}}^\dagger \cdots c_{\sigma_{N-1}}^\dagger |0\rangle \right] \quad (30)
\end{aligned}$$

where the first line corresponds to one index α in the bosonic row of the Young Tableau; the second line corresponds to one indice α in the bosonic row and one index $\alpha_i \in (\{1\dots N\} - \{A, \alpha\})$ and the third line to two indices α in the bosonic row. We note that the state $|\varphi_{int}(\alpha)\rangle$ is not normalized: we have $\langle \varphi_{int}(\alpha) | \varphi_{int}(\alpha) \rangle = 1/(2S)$.

It is now convenient to use the above decomposition rule (29) to define two initial states $|(GS, 1_A)^{\uparrow\uparrow}\rangle$ and $|(GS, 1_\alpha)^{\uparrow\downarrow}\rangle$, where the electron is added in a parallel and antiparallel spin state, respectively. $|(GS, 1_A)^{\uparrow\uparrow}\rangle$ is the state where one electron of index A at site 1 is in the parallel configuration with the ground state at site 0. It's thus the projection of $c_{1,A}^\dagger |GS\rangle$ onto its parallel part. (Here $c_{1,A}^\dagger$ is the creation operator for an electron at site 1 of index A .) We choose to give an index A to the electron at site 1 because it is already in the parallel configuration with the ground state at site 0.

$$|(GS, 1_A)^{\uparrow\uparrow}\rangle \equiv c_{1,A}^\dagger |GS\rangle . \quad (31)$$

Note that this state is normalized. $|(GS, 1_\alpha)^{\uparrow\downarrow}\rangle$ is the state where one electron of index α at site 1 is in the anti-parallel configuration with the ground state at site 0. We require $\alpha \neq A$ so that this configuration exists. We want this state to be normalized (by convention) so that

$$|(GS, 1_\alpha)^{\uparrow\downarrow}\rangle = \sqrt{\frac{2S-1}{2S}} \left[c_{1,\alpha}^\dagger |GS\rangle - c_{1,A}^\dagger |\varphi_{int}(\alpha)\rangle \right]. \quad (32)$$

3. Process 1, parallel case

In this process, one electron in the initial state $|(GS, 1_A)^{\uparrow\uparrow}\rangle$ makes a virtual incursion onto site 0 from site 1. We get the following expression for the matrix elements:

$$M_{(1)}^{\uparrow\uparrow} = t^2 \sum_{\sigma} \left| \langle GS + 1^{\uparrow\uparrow}, 0 | c_{0,\sigma}^\dagger c_{1,\sigma} | GS^{\uparrow\uparrow}, 1_A \rangle \right|^2, \quad (33)$$

where $c_{0,\sigma}^\dagger$ denotes the creation operator for an electron at site 0 of index σ and $c_{1,\sigma}$ denotes the creation operator for an electron at site 1 of index σ . $\langle GS + 1^{\uparrow\uparrow}, 0 |$ is the intermediate state, with one more electron at site 0 and no electron at site 1. By convention we suppose that both the intermediate and initial states are normalized. In the numerator in (33), we notice that $c_{0,\sigma}^\dagger c_{1,\sigma} | GS^{\uparrow\uparrow}, 1_A \rangle = \lambda | GS + 1^{\uparrow\uparrow} \rangle$, where λ is a multiplicative constant. Indeed while the electron is transferred from site two to site one it stays in the same spin configuration with respect to the impurity spin. Thus (33) can be rewritten

$$M_{(1)}^{\uparrow\uparrow} = t^2 \sum_{\sigma, \sigma'} \langle (GS, 1_A)^{\uparrow\uparrow} | c_{1,\sigma'}^\dagger c_{0,\sigma'} c_{0,\sigma}^\dagger c_{1,\sigma} | (GS, 1_A)^{\uparrow\uparrow} \rangle. \quad (34)$$

As electron at site 1 has index A , we get

$$M_{(1)}^{\uparrow\uparrow} = t^2 \langle GS | c_{0,A} c_{0,A}^\dagger | GS \rangle.$$

Then $M_{\mathbf{1}}^{\uparrow\uparrow} = \langle GS | 1 - c_{0,A}^\dagger c_{0,A} | GS \rangle$ and finally

$$M_{(1)}^{\uparrow\uparrow} = t^2 \left(1 - \frac{n_c}{2S-1+N} \right), \quad (35)$$

where $n_c/(2S-1+N)$ is the number of conduction electrons of index 1 in the ground state.

The explicit evaluation can be found in the Appendix.

4. Process 1, anti-parallel case

The initial state is $|GS^{\uparrow\downarrow}, 1_\alpha\rangle$ where one electron at site 1 is in the anti-parallel configuration with the ground state at site 0. With the same reasoning as before, we have

$$M_{(1)}^{\uparrow\downarrow} = t^2 \sum_{\sigma, \sigma'} \langle (GS, 1_\alpha)^{\uparrow\downarrow} | c_{1, \sigma'}^\dagger c_{0, \sigma'} c_{0, \sigma}^\dagger c_{1, \sigma} | (GS, 1_\alpha)^{\uparrow\downarrow} \rangle . \quad (36)$$

Remembering the electron at site 1 has index α ,

$$M_{(1)}^{\uparrow\downarrow} = t^2 \langle GS | c_{0, \alpha} c_{0, \alpha}^\dagger | GS \rangle . \quad (37)$$

Finally, as derived in the Appendix,

$$M_{(1)}^{\uparrow\downarrow} = t^2 \left(1 - \frac{n_c}{N-1} \right) . \quad (38)$$

C. Process 2, parallel case

The initial state is $|(GS, 1_\alpha)^{\uparrow\uparrow}\rangle$ where one electron at site 1 with index A is in the parallel configuration with the ground state at site 0. One electron at site 0 jumps onto site 1 and comes back.

$$M_{(2)}^{\uparrow\uparrow} = t^2 \sum_{\sigma} \left| \langle GS - 1^{\uparrow\uparrow}, 2 | c_{1, \sigma}^\dagger c_{0, \sigma} | (GS, 1_A)^{\uparrow\uparrow} \rangle \right|^2 . \quad (39)$$

As above we consider that the initial state and the intermediate state $|GS - 1^{\uparrow\uparrow}, 2\rangle$ (there is one less electron in the ground state and one more at site 1) are normalized and with the same proportionality argument,

$$\begin{aligned} M_{(2)}^{\uparrow\uparrow} &= t^2 \sum_{\sigma, \sigma'} \langle GS^{\uparrow\uparrow}, 1_A | c_{0, \sigma'}^\dagger c_{1, \sigma'} c_{1, \sigma}^\dagger c_{0, \sigma} | (GS, 1_A)^{\uparrow\uparrow} \rangle \\ &= t^2 \sum_{\sigma, \sigma'} \langle (GS, 1_A)^{\uparrow\uparrow} | c_{0, \sigma'}^\dagger \left(\delta_{\sigma, \sigma'} - c_{1, \sigma}^\dagger c_{1, \sigma} \right) c_{0, \sigma} | (GS, 1_A)^{\uparrow\uparrow} \rangle . \end{aligned} \quad (40)$$

We thus get

$$\begin{aligned} M_{(2)}^{\uparrow\uparrow} &= t^2 \sum_{\sigma} \langle (GS, 1_A)^{\uparrow\uparrow} | c_{0, \sigma}^\dagger c_{0, \sigma} | (GS, 1_A)^{\uparrow\uparrow} \rangle \\ &\quad - t^2 \langle GS | c_{0, A}^\dagger c_{0, A} | GS \rangle . \end{aligned} \quad (41)$$

We define

$$M_{(2),\sigma}^{\uparrow\uparrow} \equiv t^2 \langle GS, 1_A | c_{0,\sigma}^\dagger c_{0,\sigma} | (GS, 1_A)^{\uparrow\uparrow} \rangle - t^2 \langle GS | c_{0,A}^\dagger c_{0,A} | GS \rangle \delta_{\sigma,A} \quad (42)$$

so that $M_{(2)}^{\uparrow\uparrow} = \sum_{\sigma} M_{(2),\sigma}^{\uparrow\uparrow}$. The second term in (42) is the number of conduction electrons in the ground state that we have already calculated in (35) and which equals $n_c/(2S-1+N)$. The first term in this equation requires some exact evaluation with the expression of the state in terms of operators. After some algebra done in the Appendix, we get

$$M_{(2),\sigma}^{\uparrow\uparrow} = \begin{cases} t^2 \frac{n_c(2S+N-2)}{(N-1)(2S+N-1)} & , \sigma \neq A \\ 0 & \sigma = A \end{cases} . \quad (43)$$

An then

$$M_{(2)}^{\uparrow\uparrow} = t^2 \left(n_c - \frac{n_c}{2S+N-1} \right) . \quad (44)$$

1. Process two, anti-parallel case

The initial state is $| (GS, 1_\alpha)^{\uparrow\downarrow} \rangle$ where one electron at site 1 with index α is in the anti-parallel configuration with the ground state at site 0. Note that $\alpha \neq A$. On electron at site 0 jumps onto site 1 and comes back.

$$\begin{aligned} M_{(2)}^{\uparrow\downarrow} &= t^2 \sum_{\sigma,\sigma'} \langle (GS, 1_\alpha)^{\uparrow\downarrow} | c_{0,\sigma'}^\dagger c_{1,\sigma'} c_{1,\sigma}^\dagger c_{0,\sigma} | (GS, 1_\alpha)^{\uparrow\downarrow} \rangle \\ &= t^2 \sum_{\sigma,\sigma'} \langle (GS, 1_\alpha)^{\uparrow\downarrow} | c_{0,\sigma'}^\dagger \left(\delta_{\sigma,\sigma'} - c_{1,\sigma}^\dagger c_{1,\sigma} \right) c_{0,\sigma} | (GS, 1_\alpha)^{\uparrow\downarrow} \rangle . \end{aligned} \quad (45)$$

Remembering that the electron at site 1 has index α we get

$$M_{(2)}^{\uparrow\downarrow} = t^2 \sum_{\sigma} \langle (GS, 1_\alpha)^{\uparrow\downarrow} | c_{0,\sigma}^\dagger c_{0,\sigma} | GS^{\uparrow\downarrow}, 1_\alpha \rangle - t^2 \langle GS | c_{0,\alpha}^\dagger c_{0,\alpha} | GS \rangle . \quad (46)$$

We define

$$M_{(2),\sigma}^{\uparrow\downarrow} \equiv t^2 \langle (GS, 1_\alpha)^{\uparrow\downarrow} | c_{0,\sigma}^\dagger c_{0,\sigma} | (GS, 1_\alpha)^{\uparrow\downarrow} \rangle - t^2 \langle GS | c_{0,\alpha}^\dagger c_{0,\alpha} | GS \rangle \delta_{\sigma,\alpha} \quad (47)$$

so that $M_{(2)}^{\uparrow\downarrow} = \sum_{\sigma} M_{(2),\sigma}^{\uparrow\downarrow}$. After decomposing each state with creation operators, we get (cf. Appendix) three possibilities depending on the indices.

$$M_{(2),\sigma}^{\uparrow\downarrow} = \begin{cases} t^2 \frac{n_c}{2S + N - 1} & \sigma = A \\ 0 & \sigma = \alpha \\ t^2 \frac{n_c(2S + N - 2)}{(N - 1)(2S + N - 1)} & \text{otherwise} \end{cases}, \quad (48)$$

and after summation upon the indices we find

$$M_{(2)}^{\uparrow\downarrow} = t^2 \left(n_c - \frac{n_c}{N - 1} + \frac{n_c}{(N - 1)(2S + N - 1)} \right). \quad (49)$$

2. Energy shifts

We evaluate the energy shifts with the expression

$$\Delta E^{\uparrow\uparrow} - \Delta E^{\uparrow\downarrow} = \frac{M_{(1)}^{\uparrow\uparrow}}{E(n_e) - E^{\uparrow\uparrow}(n_e + 1)} - \frac{M_{(1)}^{\uparrow\downarrow}}{E(n_e) - E^{\uparrow\downarrow}(n_e + 1)} + \frac{M_{(2)}^{\uparrow\downarrow} - M_{(2)}^{\uparrow\uparrow}}{E(n_e) - E(n_e - 1)} \quad (50)$$

and we get

$$\Delta E^{\uparrow\uparrow} - \Delta E^{\uparrow\downarrow} = \frac{t^2}{J} \left[\frac{n_f N}{(N - 1)(N - n_f^* - Q/N)} - \frac{QN}{(Q + N - n_f^*)(N + Q + 1 - 2n_f^* - Q/N)} - \frac{(N - n_f^*)(Q - n_f^*)N}{(n - 1)(Q + N - n_f^*)(n_f^* + Q/N)} \right]. \quad (51)$$

where we have put $n_f^* = n_f + 1$, in keeping with our initial definition of L-shaped Young tableaux. This expression is valid for any (Q, n_f^*, N) .

In the large N limit when $Q/N = q$, $n_f^*/N = \tilde{n}_f$ and $(2S + 1)/N = \tilde{n}_b$, we get

$$\Delta E^{\uparrow\uparrow} - \Delta E^{\uparrow\downarrow} = \frac{t^2}{J} \left[\frac{\tilde{n}_f}{1 - \tilde{n}_f} - \frac{1 - \tilde{n}_f}{\tilde{n}_f} - \frac{1}{\tilde{n}_b + 1} \left(\frac{q}{\tilde{n}_b + 1 - \tilde{n}_f} - \frac{1 - \tilde{n}_f}{\tilde{n}_f} \right) \right]. \quad (52)$$

Reducing to the same denominator and dividing by \tilde{n}_b in order to get the effective coupling (23), we finally have

$$J^* = -\frac{t^2}{J(1 - \tilde{n}_f)\tilde{n}_f} \left[\frac{\frac{1}{2} - \tilde{n}_f}{(1 - \tilde{n}_f + \tilde{n}_b)} \right]. \quad (53)$$

In the next section, we will check this result in the framework of the large N approach, using the formalism of paper³.

III. STRONG COUPLING IN THE LARGE N APPROACH

In order to test the formalism developed in³, we need to rederive the effective coupling constant J^* in the large N limit with the path integral formulation.

A. Mean-Field theory

The impurity is described within a $SU(N)$ representation in form of a L-shaped Young Tableau. The impurity Kondo model is written

$$H = \overbrace{\sum_{k,\alpha} \epsilon_k c_{k\alpha}^\dagger c_{k\alpha}}^{H_o} + \overbrace{\frac{J}{N} c_\alpha^\dagger \mathbf{\Gamma}_{\alpha\beta} c_\beta \cdot \mathbf{S}}^{H_K} + \overbrace{\lambda(Q - Q_0)}^{H_Q} + \overbrace{+\zeta(\mathcal{Y} - Y_o) \frac{\zeta}{Q_o} \hat{Q} \hat{\mathcal{Y}}}_{H_Y}, \quad (54)$$

where H_o describes the conduction electron sea, H_K is the interaction between the conduction electron spin density, and the local moment, where $c_\alpha^\dagger = n_s^{-1/2} \sum_k c_{k\alpha}^\dagger$ creates an electron at the site of the local moment ($n_s =$ no. of sites). H_Q and H_Y impose the constraints given by $\hat{Q} = n_f + n_b = Q_o$ and $\hat{\mathcal{Y}} = n_f - n_b + \frac{1}{Q} [b_\alpha^\dagger f_\alpha = Y_o, f_\beta^\dagger b_\beta]$. n_f and n_b are respectively the number of f-electrons and bosons which parametrize the representation.

In the strong coupling limit, this Hamiltonian becomes

$$H = -\frac{J}{N} \sum_{\alpha\beta} f_\alpha^\dagger c_\alpha c_\beta^\dagger f_\beta - \frac{J}{N} \sum_{\alpha\beta} b_\alpha^\dagger c_\alpha c_\beta^\dagger b_\beta + \lambda(Q - Q_0) + \zeta(\mathcal{Y} - Y_o). \quad (55)$$

After factorizing the Kondo interaction, we obtain

$$H = \sum_\sigma \left(c_\sigma^\dagger \bar{V} f_\sigma + f_\sigma^\dagger V c_\sigma \right) + \sum_\sigma \left(c_\sigma^\dagger b_\sigma \alpha + \bar{\alpha} b_\sigma^\dagger c_\sigma \right) + \frac{N}{J} (\bar{V} V - \bar{\alpha} \alpha) + \lambda(Q - Q_0) + \zeta(\mathcal{Y} - Y_o)$$

At the large N saddle point, the fluctuating variable V acquires a static value, which we take to be $\langle V \rangle = \langle \bar{V} \rangle = V$. The average value of the Grassman field α is zero, so the Bose field is unhybridized in the large N limit. In order that $n_b \sim 0(N)$, the Bose field must

condense so that the chemical potential of the Bose field, $\lambda_b = \lambda - \zeta$ must vanish, i.e. $\lambda = \zeta$.

The mean-field Hamiltonian is then

$$H_{MF} = H = \sum_{\sigma} V \left(c_{\sigma}^{\dagger} f_{\sigma} + f_{\sigma}^{\dagger} c_{\sigma} \right) + \frac{N}{J} V^2 + 2\zeta n_f - 2\zeta Q_o - \zeta Y_o, \quad (56)$$

where the interaction term entering into \mathcal{Y} is ignored at this level of approximation. After diagonalization of the Fermionic Hamiltonian, we find two eigenvalues $E_{\pm} = \zeta \pm \sqrt{\zeta^2 + V^2}$ and the ground state hamiltonian can be written

$$H_{GS} = \sum_{\sigma} (E_{+} a_{+ \sigma}^{\dagger} a_{+ \sigma} + E_{-} a_{- \sigma}^{\dagger} a_{- \sigma}) + 2N \frac{V^2}{J} - 2\zeta N \tilde{n}_f. \quad (57)$$

where $a_{\pm \sigma} = \frac{1}{\sqrt{2}}(c_{\sigma} \pm f_{\sigma})$ and $\tilde{n}_f = n_f/N$. The ground-state corresponds to complete occupation of all N states in the lowest level, so that the ground-state energy is

$$E_{GS} = N \left(\zeta - \sqrt{\zeta^2 + V^2} + \frac{V^2}{J} - 2\zeta \tilde{n}_f \right). \quad (58)$$

Minimizing E_{GS} with respect to ζ and V^2 gives the two saddle-point equations

$$1 - \frac{\zeta}{\sqrt{\zeta^2 + V^2}} = 2\tilde{n}_f$$

$$\frac{1}{2\sqrt{\zeta^2 + V^2}} = \frac{1}{J}, \quad (59)$$

so that

$$J = 2\sqrt{\zeta^2 + V^2}$$

$$\zeta = J(1 - 2\tilde{n}_f). \quad (60)$$

These are the mean-field equations of the strong coupling fixed point. Substituting back into equation (58), we obtain

$$E_{GS} = -NJ\tilde{n}_c\tilde{n}_f \quad (61)$$

where $\tilde{n}_c = n_c/N = 1 - \tilde{n}_f$ is the number of conduction electrons in the ground-state.

B. Excitation energies

Suppose now that we want to describe the excitation energies of the large N limit, to compare with those obtained in a direct strong-coupling expansion (25). In the mean-field, the energy level E_- is completely filled. If we add electrons to the impurity, they must go into the upper level. We can add a large number of electrons into this level, so we identify this excitation with the “anti-parallel” excitation states, giving an excitation energy

$$\begin{aligned}\Delta E^\perp = E_+ &= \zeta + \sqrt{\zeta^2 + V^2} \\ &= J(1 - \tilde{n}_f).\end{aligned}\tag{62}$$

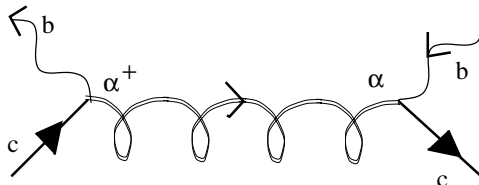
This matches the large N limit of eq. (25). The leading large N calculation is able to capture the energy to add an electron into an “anti-parallel” configuration because one can add many electrons into these states, giving an energy change of order $O(N)$. By contrast, one can no more than one electron in the parallel spin configuration, since it is not possible to symmetrize more than one electron at a given site. In this case, the change in energy is of order $O(1)$, and we must consider the Gaussian corrections to the mean-field theory to extract this excitation energy.

C. Gaussian fluctuations

The most important fluctuations about the mean-field theory, are the fluctuations of the α -field. The relevant interaction part of the Lagrangian is given by

$$\mathcal{L}_\alpha = \sum_\sigma (c_\sigma^\dagger b_\sigma \alpha + \bar{\alpha} b_\sigma^\dagger c_\sigma) - \frac{N}{J} \bar{\alpha} \alpha .$$

Fluctuations of the alpha field thus mediate an interaction between the partially screened moment and the conduction electrons, given by



where the full line denotes a conduction electron propagator, $G_c^{-1}(\omega) = (\omega - \frac{V^2}{\omega - 2\zeta})$, a wavy line indicates a boson propagator $G_b^{-1}(\nu) = (\nu - \lambda_b)$, where $\lambda_b = \lambda - \zeta$ is the chemical potential of the Bose field and a curly line indicates the α propagator. Poles in this propagator describe excitations associated with the action of the operator $c_o^\dagger b_\sigma$ on the ground-state. But since $\langle b_\sigma \rangle = \sqrt{n_b} \delta_{A\sigma}$, this operator describes the addition of an electron into a parallel spin configuration with the unscreened local moment. Thus, to find out the energy to add an electron to the spin in the “parallel” spin configuration, we must look for poles in the α propagator. The action for the α fluctuations is given by

$$S_{fluc} = -N \sum_{\omega} \bar{\alpha}(\omega) D^{-1}(\omega) \alpha(\omega) \quad (63)$$

where

$$D^{-1}(\omega) = \frac{1}{J} + T \sum_{\nu} G_c(\omega + \nu) G_b(\nu) , \quad (64)$$

Now stationarity of the action with respect to the quantity V gives

$$\frac{\partial F}{\partial V} = \frac{V}{J} + T \sum_{\omega} G_c(\omega) \frac{V}{\omega - 2\zeta} = 0$$

Using this to replace $1/J$ in the inverse propagator , we obtain

$$D^{-1}(\omega) = T \sum_{\nu} G_c(\omega + \nu) \left(\frac{1}{\nu - \lambda_b} - \frac{1}{\nu + \omega - 2\zeta} \right) . \quad (65)$$

Carrying out this sum using the contour-integral method, we obtain

$$\begin{aligned} \frac{D^{-1}(\omega)}{(\omega - 2\zeta)} &= - \oint \left[\frac{dz n_b(z)}{2\pi i} \frac{1}{(z - \lambda_b)(z + i\omega_n - E_+)(z + i\omega_n - E_-)} \right] \\ &= - \left[\frac{n_b(\lambda_b)}{(\omega - E^+)(\omega - E^-)} + \sum_{\alpha=\pm} \frac{-f(E_\alpha)}{(E_\alpha - \omega)(E_\alpha - E_{-\alpha})} \right] \\ &= - \sum_{\alpha} \frac{\tilde{n}_b - f(E_\alpha)}{(\omega - E_\alpha)(E_\alpha - E_{-\alpha})} . \end{aligned} \quad (66)$$

But at $T = 0$, $f(E_-) = 1$ and $f(E^+) = 0$ which leads to

$$D^{-1}(\omega) = \left[\frac{-\tilde{n}_b}{\omega - E_+} + \frac{1 + \tilde{n}_b}{\omega - E_-} \right] \frac{(\omega - 2\zeta)}{2\sqrt{V^2 + \zeta^2}}$$

so that finally

$$D^{-1}(\omega) = \frac{\omega - \omega^*}{(\omega - E_+)(\omega - E_-)} \frac{(\omega - 2\zeta)}{2\sqrt{V^2 + \zeta^2}} \quad (67)$$

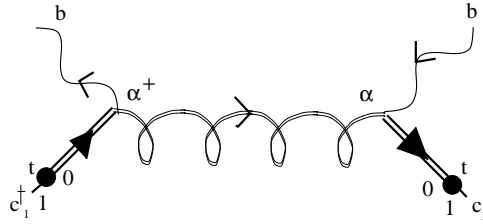
where $\omega^* = E_+ + J\tilde{n}_b$. Notice, that $D(\omega)$ has poles at both $\omega = \omega^*$ and $\omega = 2\zeta$. The appearance of a second pole at $\omega = 2\zeta$ is a “ghost” which factors out of the entire partition function when we fix the gauge properly³, and it does not contribute to physical excitations. We can identify the excitation energy

$$\Delta E_{\perp} = \omega^* = J(1 - \tilde{n}_f + \tilde{n}_b)$$

as the physical energy to add an electron in the perpendicular spin configuration. This result agrees with the large N limit of result (22). result defines the pole in the α propagator.

D. Renormalized Spin Interaction between conduction electrons and residual spin.

The residual interaction between the partially quenched moment and the electrons at site “1” is given in strong-coupling by the diagram



where the “ t ” denotes the hopping matrix element for an electron moving between site 1 and site 0. In this diagram, the external legs do not contribute to the interaction amplitude. The total interaction strength at low energies is consequently

$$\frac{J^*}{N} = t^2 [G_c(\omega)]^2 D(\omega)|_{\omega=0} \quad (68)$$

where

$$G_c(\omega) = \frac{1}{\omega - \frac{V^2}{\omega - 2\zeta}} \quad (69)$$

is the propagator for a conduction electron at site 0. At zero frequency, we have

$$G_c(\omega) = \frac{2\zeta}{V^2} \quad (70)$$

From eq (67), we have

$$D(0) = -\frac{2\zeta\omega^*}{JV^2} \quad (71)$$

so that

$$J^* = -\frac{Jt^2(2\zeta)}{2\omega^*V^2} . \quad (72)$$

Now using the mean-field equations, we get

$$\begin{aligned} \omega^* &= J(1 - \tilde{n}_f + \tilde{n}_b) \\ \frac{V^2}{2\zeta} &= \frac{1 - 2\tilde{n}_f}{J^2\tilde{n}_f(1 - \tilde{n}_f)} \end{aligned}$$

so that finally

$$J^* = -\frac{t^2(1/2 - \tilde{n}_f)}{J(1 - \tilde{n}_f)\tilde{n}_f(1 - \tilde{n}_f + \tilde{n}_b)} . \quad (73)$$

This result corresponds to the result obtained using a direct strong coupling expansion (53).

IV. CONCLUSION

In this paper we have investigated the effect of the representation in the description of the SU(N) Kondo model. We used a special class of Young tableaux which are L-shaped and we obtain a path integral expression of our model with an additional symmetry between fermions and bosons: the supersymmetry. This formalism enables us to tune the Hund's interactions inside the representation, which can be used to describe complex atoms like U^{3+} .

We have found that changing the representation gives rise to new fixed points in the physics of the Kondo model. When the number of fermions (antisymmetric components in the L-shaped Young tableau) is larger than $N/2$ (in the large N limit), then a two-stage

Kondo appears, where the impurity spin is screened twice by two clouds of conduction electrons, leading to a resulting spin of $S^* = S - 1$. In addition to the two-stage Kondo effect, a class of representations (where for example $n_b^* = 2$ and $n_f^* = N - 1$) lead to a degenerate ground state and thus to a non fermi liquid. We didn't investigate so far the properties of this new fixed point.

Alternatively, this paper is a test for the formalism developed in our previous work about a large N field theory for the $SU(N)$ Kondo model. We have given here the full renormalization group argument to prove the unstability of the fixed point leading to the two-stage Kondo effect. We have matched the unstability criterions in the limit of large N . The excitation energies involved in adding an extra electron to the screened impurity both in the parallel and anti-parallel states have been reproduced.

APPENDIX A: SOME DETAILED EVALUATIONS

1. The norm of the ground state

We illustrate the use of the notation in formula 28 by checking that $\langle GS|GS\rangle = 1$. Using the relation $\langle 0|b_A^{2S}b_A^\dagger{}^{2S}|0\rangle = (2S)!$ we have

$$\begin{aligned} \langle GS|GS\rangle = \frac{1}{N_{GS}^2} & \left[(2S)! \binom{N-1}{n_f} (n_f!)^2 (n_c!)^2 \right. \\ & \left. + (2S-1)!(N-1) \binom{N-1}{n_f} (n_f!)^2 (n_c!)^2 \right] \end{aligned} \quad (A1)$$

so that

$$\langle GS|GS\rangle = \frac{1}{N_{GS}^2} (2S + N - 1)(2S - 1)! \binom{N-1}{n_f} (n_f!)^2 (n_c!)^2 = 1 \quad (A2)$$

2. Number of conduction electrons of different indices in the ground state

a. Number of electrons of index 1

In the equation 28 there are no c-electrons of index 1 in the first line. We thus get

$$c_1|GS\rangle = \frac{1}{N_{GS}} \sum_{\sigma_i \neq A} (b_A^\dagger)^{2S-1} b_{\sigma_i}^\dagger \sum_{\tilde{S}_{n_f} \in (\{1\dots N\} - \{A, \sigma_i\})} \varepsilon' f_{\sigma_1}^\dagger \cdots f_{\sigma_{n_f}}^\dagger c_{\sigma_{n_f+1}}^\dagger \cdots c_{\sigma_{N-1}}^\dagger |0\rangle. \quad (\text{A3})$$

The choice of indices for the f-electrons can not be 1 any more because it is attributed to the c-electron in that sum. Noting $n_{c_A} = \langle GS | c_A^\dagger c_A | GS \rangle$ we get

$$\begin{aligned} n_{c_A} &= \frac{(N-1) \binom{n_f}{N-2}}{(2S+N-1) \binom{N-1}{n_f}} \\ &= \frac{n_c}{(2S+N-1)}, \end{aligned} \quad (\text{A4})$$

where n_c is the total number of c-electrons in the ground state.

b. Number of electrons of index $\sigma \neq A$ in the ground state

$$\begin{aligned} c_\sigma |GS\rangle &= \frac{1}{N_{GS}} \left[(b_A^\dagger)^{2S-1} n_f! n_c! \sum_{\tilde{S}_{n_f} \in (\{1\dots N\} - \{A, \sigma\})} \varepsilon' f_{\sigma_1}^\dagger \cdots f_{\sigma_{n_f}}^\dagger c_{\sigma_{n_f+1}}^\dagger \cdots c_{\sigma_{N-1}}^\dagger |0\rangle \right. \\ &\quad \left. + \sum_{\sigma_i \neq \sigma} (b_A^\dagger)^{2S-1} b_{\sigma_i}^\dagger \sum_{\tilde{S}_{n_f} \in (\{1\dots N\} - \{\sigma, \sigma_i\})} \varepsilon' f_{\sigma_1}^\dagger \cdots f_{\sigma_{n_f}}^\dagger c_{\sigma_{n_f+1}}^\dagger \cdots c_{\sigma_{N-1}}^\dagger |0\rangle \right]; \end{aligned} \quad (\text{A5})$$

Thus we get

$$\begin{aligned} n_{c\sigma} &= \frac{1}{N_{GS}^2} \left[(2S+N-2) \binom{n_f}{N-2} (2S-1)! (n_f! n_c!)^2 \right] \\ &= \frac{n_c (2S+N-2)}{(2S+N-1)(N-1)}. \end{aligned} \quad (\text{A6})$$

We note that summing over the indices, we can check that the total number of conduction electrons in the ground state is equal to $n_c = N - n_f - 1$.

3. Process 1, anti-parallel case: evaluation of the matrix element

The electron at site 1 has index $\alpha \neq A$.

$$|GS^{\uparrow\downarrow}, 1_\alpha\rangle = \sqrt{\frac{2S-1}{2S}} \left[c_{1,\alpha}^\dagger |GS\rangle - c_{1,A}^\dagger |\varphi_{int}(\alpha)\rangle \right], \quad (\text{A7})$$

where we have noted $c_{1,\alpha}^\dagger$ the creation operator for an electron of index α at site 1. Due to the presence of the electron at site 1 the two state in A7 are anti-parallel. We get

$$\begin{aligned}
\langle GS^{\uparrow\downarrow}, 1 | GS^{\uparrow\downarrow}, 1 \rangle &= \frac{2S-1}{2S} \left[\langle GS | c_{1,\alpha} c_{1,\alpha}^\dagger | GS \rangle + \langle \varphi_{int}(\alpha) | c_{1,A} c_{1,A}^\dagger | \varphi_{int}(\alpha) \rangle \right] \\
&= \frac{2S-1}{2S} \left[\langle GS | GS \rangle + \langle \varphi_{int}(\alpha) | \varphi_{int}(\alpha) \rangle \right] \\
&= 1 .
\end{aligned} \tag{A8}$$

Now starting from eq. 37 the full matrix element for this case is given by

$$\begin{aligned}
M_{(1)}^{\uparrow\downarrow} &= t^2 \frac{2S-1}{2S} \left[\langle GS | 1 - c_\alpha^\dagger c_\alpha | GS \rangle + \langle \varphi_{int} | 1 - c_A^\dagger c_A | \varphi_{int} \rangle + 2 \langle \varphi_{int} | c_\alpha^\dagger c_A | GS \rangle \right] \\
&= t^2 \frac{2S-1}{2S} \left[1 - \frac{n_c(2S)}{(2S+N-1)(N-1)} + \frac{1}{2S-1} \left(1 - \frac{n_c N}{(2S+N-1)(N-1)} \right) + 2 \frac{n_c}{(2S+N-1)(N-1)} \right] \\
&= t^2 \left(1 - \frac{n_c}{N-1} \right) .
\end{aligned}$$

4. Process 2, parallel case: evaluation of the matrix element

We suppose that the electron at site 1 has index A. From eq. 41 it is clear that if the hopping electron had index $\sigma = A$ the corresponding matrix element vanishes. For a hopping electron with index $\sigma \neq A$, we can study the state $|(GS, 1_A)^{\uparrow\uparrow}\rangle$ in the first term of eq. 41.

We have

$$\begin{aligned}
|(GS, 1_A)^{\uparrow\uparrow}\rangle &= \frac{1}{N_{GS}} \left[(b_A^\dagger)^{2S-1} n_f! n_c! \sum_{\tilde{S}_{n_f} \in \{1\dots N\} - \{A\}} \varepsilon' f_{\sigma_1}^\dagger \cdots f_{\sigma_{n_f}}^\dagger c_{2,A}^\dagger c_{\sigma_{n_f+1}}^\dagger \cdots c_{\sigma_{N-1}}^\dagger |0\rangle \right. \\
&\quad \left. + \sum_{\sigma_i \neq A} (b_A^\dagger)^{2S-1} b_{\sigma_i}^\dagger \sum_{\tilde{S}_{n_f} \in (\{1\dots N\} - \{\sigma_i\})} \varepsilon' f_{\sigma_1}^\dagger \cdots f_{\sigma_{n_f}}^\dagger c_{2,A}^\dagger c_{\sigma_{n_f+1}}^\dagger \cdots c_{\sigma_{N-1}}^\dagger |0\rangle \right] . \tag{A10}
\end{aligned}$$

Thus for $\sigma \neq A$ we get

$$\begin{aligned}
c_\sigma |(GS, 1_A)^{\uparrow\uparrow}\rangle &= \frac{1}{N_{GS}} \left[(b_A^\dagger)^{2S-1} n_f! n_c! \sum_{\tilde{S}_{n_f} \in (\{1\dots N\} - \{A, \sigma\})} \varepsilon' f_{\sigma_1}^\dagger \cdots f_{\sigma_{n_f}}^\dagger c_{2,A}^\dagger c_{\sigma_{n_f+1}}^\dagger \cdots c_{\sigma_{N-1}}^\dagger |0\rangle \right. \\
&\quad \left. + \sum_{\sigma_i \neq A} (b_A^\dagger)^{2S-1} b_{\sigma_i}^\dagger \sum_{\tilde{S}_{n_f} \in (\{1\dots N\} - \{\sigma, \sigma_i\})} \varepsilon' f_{\sigma_1}^\dagger \cdots f_{\sigma_{n_f}}^\dagger c_{2,A}^\dagger c_{\sigma_{n_f+1}}^\dagger \cdots c_{\sigma_{N-1}}^\dagger |0\rangle \right] \tag{A11}
\end{aligned}$$

and when taking the norm we get

$$M_{(2),\sigma}^{\uparrow\uparrow} = t^2 \frac{n_c(2S+N-2)}{(N-1)(2S+N-1)} \quad \text{if } \sigma \neq A \tag{A12}$$

5. Process 2, anti-parallel case: evaluation of the matrix element

In this process we choose on site 1 an electron with an index $\alpha \neq A$. The second term in eq. 46 corresponds to the number of c-electrons of index $\alpha \neq 1$ in the ground state which has been evaluated in section A 2 a. We study the first term in eq. (46). We have three different cases.

a. $\sigma \neq \alpha$ and $\sigma \neq A$

$$c_\sigma |GS^{\uparrow\downarrow}, 1_\alpha\rangle = -\sqrt{\frac{2S-1}{2S}} \left[c_{1,\alpha}^\dagger c_\sigma |GS\rangle - c_{1,A}^\dagger c_\sigma |\varphi_{int}(\alpha)\rangle \right]. \quad (\text{A13})$$

We then have the two states

$$\begin{aligned} c_\sigma |GS\rangle &= \frac{1}{N_{GS}} \left[(b_A^\dagger)^{2S-1} n_f! n_c! \sum_{\tilde{S}_{n_f} \in (\{1\dots N\} - \{A, \sigma\})} \varepsilon' f_{\sigma_1}^\dagger \cdots f_{\sigma_{n_f}}^\dagger c_{\sigma_{n_f+1}}^\dagger \cdots c_{\sigma_{N-1}}^\dagger |0\rangle \right. \\ &\quad \left. + \sum_{\sigma_i \neq A} (b_A^\dagger)^{2S-1} b_{\sigma_i}^\dagger \sum_{\tilde{S}_{n_f} \in (\{1\dots N\} - \{\sigma, \sigma_i\})} \varepsilon' f_{\sigma_1}^\dagger \cdots f_{\sigma_{n_f}}^\dagger c_{\sigma_{n_f+1}}^\dagger \cdots c_{\sigma_{N-1}}^\dagger |0\rangle \right]; \quad (\text{A14}) \end{aligned}$$

and

$$\begin{aligned} c_\sigma |\varphi_{int}(\alpha)\rangle &= \frac{1}{N_{GS}} \left[\binom{N-1}{n_f} n_f! n_c! (b_A)^{2S-1} b_\sigma^\dagger \sum_{\tilde{S}_{n_f} \in (\{1\dots N\} - \{A, \sigma\})} \varepsilon' f_{\sigma_1}^\dagger \cdots f_{\sigma_{n_f}}^\dagger c_{\sigma_{n_f+1}}^\dagger \cdots c_{\sigma_{N-1}}^\dagger |0\rangle \right. \\ &\quad + \sum_{\sigma_i \in (\{1\dots N\} - \{A, \sigma\})} \binom{N-1}{n_f} n_f! n_c! (b_A)^{2S-2} b_\sigma^\dagger b_{\sigma_i}^\dagger \sum_{\tilde{S}_{n_f} \in (\{1\dots N\} - \{A, \sigma\})} \varepsilon' f_{\sigma_1}^\dagger \cdots f_{\sigma_{n_f}}^\dagger c_{\sigma_{n_f+1}}^\dagger \cdots c_{\sigma_{N-1}}^\dagger |0\rangle \\ &\quad \left. + \binom{N-1}{n_f} n_f! n_c! (b_A^\dagger)^{2S-2} (b_\sigma^\dagger)^2 \sum_{\tilde{S}_{n_f} \in (\{1\dots N\} - \{A, \sigma\})} \varepsilon' f_{\sigma_1}^\dagger \cdots f_{\sigma_{n_f}}^\dagger c_{\sigma_{n_f+1}}^\dagger \cdots c_{\sigma_{N-1}}^\dagger |0\rangle \right]. \quad (\text{A15}) \end{aligned}$$

For $\sigma \neq \alpha$ these two states are anti-parallel and we get

$$\begin{aligned} \langle GS | c_{0,\sigma}^\dagger c_{1,\alpha} c_{1,\alpha}^\dagger c_{0,\sigma} | GS \rangle &= \frac{n_c(2S+N-2)}{(N-1)(2S+N-1)} \\ \langle \varphi_{int}(\alpha) | c_{0,\sigma}^\dagger c_{1,\alpha} c_{1,\alpha}^\dagger c_{0,\sigma} | \varphi_{int}(\alpha) \rangle &= \frac{n_c(2S+N-2)}{2S(N-1)(2S+N-1)} \end{aligned} \quad (\text{A16})$$

so that we get

$$M_{(2),\sigma}^{\uparrow\downarrow} = t^2 \frac{n_c(2S+N-2)}{(N-1)(2S+N-1)} \quad \text{if } \sigma \neq \alpha \text{ and } \sigma \neq A \quad (\text{A17})$$

b. $\sigma = A$

The two states in eq. A13 are still anti-parallel in that case. We have

$$c_A |GS\rangle = \frac{1}{N_{GS}} \sum_{\sigma_i \neq A} (b_A^\dagger)^{2S-1} b_{\sigma_i}^\dagger \sum_{\tilde{S}_{n_f} \in (\{1\dots N\} - \{A, \sigma_i\})} \varepsilon' f_{\sigma_1}^\dagger \cdots f_{\sigma_{n_f}}^\dagger c_{\sigma_{n_f+1}}^\dagger \cdots c_{\sigma_{N-1}}^\dagger |0\rangle ; \quad (\text{A18})$$

$$\begin{aligned} c_A |\varphi_{int}(\alpha)\rangle = \frac{1}{N_{GS}} & \left[\sum_{\sigma_i \in \{1\dots N\} - \{A\}} \binom{N-1}{n_f} n_f! n_c! (b_A)^{2S-2} b_\sigma^\dagger b_{\sigma_i}^\dagger \sum_{\tilde{S}_{n_f} \in \{1\dots N\} - \{A\}} \varepsilon' f_{\sigma_1}^\dagger \cdots f_{\sigma_{n_f}}^\dagger c_{\sigma_{n_f+1}}^\dagger \cdots c_{\sigma_{N-1}}^\dagger |0\rangle \right. \\ & \left. + \binom{N-1}{n_f} n_f! n_c! (b_A^\dagger)^{2S-2} (b_\sigma^\dagger)^2 \sum_{\tilde{S}_{n_f} \in \{1\dots N\} - \{A\}} \varepsilon' f_{\sigma_1}^\dagger \cdots f_{\sigma_{n_f}}^\dagger c_{\sigma_{n_f+1}}^\dagger \cdots c_{\sigma_{N-1}}^\dagger |0\rangle \right] \end{aligned}$$

As a result we get

$$M_{(2),A}^{\uparrow\downarrow} = t^2 \frac{n_c}{2S + N - 1} \quad (\text{A20})$$

c. $\sigma = \alpha$

It is easy from eq. 46 to check that in this case $M_{\alpha,(2)}^{\uparrow\downarrow} = 0$.

REFERENCES

- ¹ D. L. Cox and M. Makivic, *Physica B* **199-200**, 391 (1994).
- ² M. Norman, *Phys. Rev. Lett*, **72**, 2077 (1994).
- ³ P. Coleman, C. Pépin and A. M. Tsevlík cond-mat 9909073
- ⁴ Ph. Nozières and A. Blandin, *J. Phys. (Paris)* **41**, 193 (1980).
- ⁵ B. Coqblin, J. R. Schrieffer, *Phys. Rev.* **185**, 847 (1969).
- ⁶ For a reference on Young tableaux, see e.g. M Hammermesh, “Group theory and its Application to Physical problems”, pp 198, Addison Wesley, (1962); or Lichtenberg “Unitary Symmetry and elementary particle”, Academic Press (New York and London) or H.F. Jones, “Groups Representations and Physics”, Institute of Physics, (1990).
- ⁷ N. Andrei, K. Furuya and J. H. Lowenstein, *Rev. Mod. Phys.*, **55**, (1983).
- ⁸ A. M. Tselik and P. B. Weigman, *J. Phys C: Solid State Physics* **15**,1707 (1984).
- ⁹ D. M. Newns and N. Read, *J. Phys C.: Solid State Physics* **29**, L1055, (1983).
- ¹⁰ P. Coleman and N. Andrei, *J. Phys C.: Solid State Physics* **19**, 3211 (1986).
- ¹¹ P. Coleman, *Phys. RevB* **35**, 5073 1987).
- ¹² I. Affleck and A. Ludwig, *Phys Rev. B* **48** 7297 (1993) and references therein.
- ¹³ O. Parcollet and A. Georges, *Phys. Rev. Lett* **79**, 4665 (1997).
- ¹⁴ O. Parcollet, A. Georges, G. Kotliar and A. Sengupta, *Phys. Rev. B.* **50**, 3794 (1998).
- ¹⁵ P. W. Anderson, *Phys. Rev.* **164**, 352 (1967).
- ¹⁶ P. Nozières, *J. Phys. (Paris) Colloq.* **37**, C1-271 (1976).
- ¹⁷ A. M. tselik and P. B. Wiegmann, *J. Stat. Phys.* **38**, 125 (1985); A. M. Tselik, *J. Phys. C* **18**, 159 (1985).

¹⁸ C. Destri and N. Andrei, Phys. Rev. Lett **52**, 364 (1984).

¹⁹ K. G. Wilson, Rev. Mod. Phys. **47**, 773 (1975).

²⁰ A. Jerez, N. Andrei and G. Zarand, Phys. Rev. B **58**,3814 (1998).